

CFAR processing with switching exponential smoothers for nonhomogeneous environments

Berk Gurakan*, Çağatay Candan, Tolga Çiloğlu

Department of Electrical and Electronics Engineering, METU, Ankara, Turkey

ARTICLE INFO

Article history:

Available online 1 February 2012

Keywords:

CFAR detection
Nonhomogeneous clutter
Exponential smoother

ABSTRACT

Conventional constant false alarm rate (CFAR) methods use a fixed number of cells to estimate the background variance. For homogeneous environments, it is desirable to increase the number of cells, at the cost of increased computation and memory requirements, in order to improve the estimation performance. For nonhomogeneous environments, it is desirable to use less number of cells in order to reduce the number of false alarms around the clutter edges. In this work, we present a solution with two exponential smoothers (first order IIR filters) having different time-constants to leverage the conflicting requirements of homogeneous and nonhomogeneous environments. The system is designed to use the filter having the large time-constant in homogeneous environments and to promptly switch to the filter having the small time constant once a clutter edge is encountered. The main advantages of proposed Switching IIR CFAR method are computational simplicity, small memory requirement (in comparison to windowing based methods) and its good performance in homogeneous environments (due to the large time-constant smoother) and rapid adaptation to clutter edges (due to the small time-constant smoother).

© 2012 Elsevier Inc. All rights reserved.

1. Introduction

Maintaining a constant false alarm rate (CFAR) is an important task especially for modern radar systems which can simultaneously follow a multitude of targets while conducting a search for newly emerging ones. This task is, in general, accomplished by adaptive receivers. Adaptive receivers estimate the disturbance level by processing some auxiliary data and adjust the detection threshold accordingly to ensure a constant false alarm rate. Conventional CFAR systems use a finite number of samples around the cell of interest for this purpose. It is well known that a better estimate of the disturbance level can be produced with a larger number of samples provided that the statistics of the environment stays the same, i.e. in homogeneous environments. For nonhomogeneous environments, increasing the number of samples does not immediately result in a performance improvement. A large number of CFAR techniques have been proposed in the literature to improve the estimation performance in nonhomogeneous environments with a negligible loss of performance in the homogeneous case.

In this paper, we present a CFAR technique with very low computational and memory requirements, which is especially suitable for real-time embedded applications. The proposed technique uses two exponential smoothers (first order IIR filters) with different time-constants to estimate the disturbance level. In homogeneous

environments, the estimator with larger time-constant (which we call as the ‘slow filter’) is utilized to provide a highly accurate estimate of the disturbance level based on a long-term average. In nonhomogeneous environments, the system switches to the fast filter, which has a much smaller time-constant, as soon as an abrupt change, such as a clutter edge, is encountered. This system is causal and has the memory requirement of a single accumulator and the computational requirement of 2 multiplications per output sample for each filter. In this paper, we examine the performance of the described system in different environments.

In the literature, many CFAR systems have been proposed. The first example of a CFAR detector can be found in Finn and Johnson [1] where an arithmetic mean detector, namely, Cell Averaging CFAR (CA-CFAR) is analyzed. This detector is shown to be optimal in the presence of spatially homogeneous environment but its performance degrades significantly at multiple target situations [2] and at the clutter edges [3]. Some robustness against nonhomogeneous environments can be attained by order-statistics (OS) based CFAR algorithms [4].

In addition to the order-statistics based methods, data censoring has been applied to lessen the effect of the inhomogeneities in the collected data. Fixed censoring methods such as Censored Mean Level Detector (CMLD) [2] are effective against multiple targets, however, a priori information is required for the proper censoring of the outliers. This led to the development of automatic censoring methods such as A-CMLD and GTL-CMLD [5]. Recently, the concept of variability index is introduced in [6] and this idea

* Corresponding author.

E-mail address: berkgurakan@gmail.com (B. Gurakan).

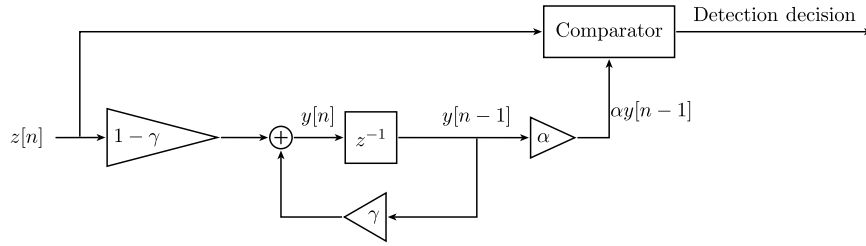


Fig. 1. Detection using an IIR filter.

is incorporated in automatic censoring [7,8]. Other methods based on Fuzzy CFAR detectors have also been proposed in [9–11].

Conventional CFAR methods, such as the ones mentioned above, utilize a set of reference samples around a test cell for background estimation and to declare the presence or the absence of the target. The detection threshold is formed by the elements of the reference set and then the cell under test is compared with this threshold. The process is repeated for all test cells of interest. Typically, a sliding window containing the reference and the test cells are utilized for this purpose. Sliding windows require data storage of at least the number of cells in the window, which can be a significant requirement for many practical systems. The storage requirement can be reduced by using an exponential smoothing filter [12].

The background estimate with an exponential smoothing filter $y[n]$ is formed by a weighted average of the square law detected range samples $z[n]$ and the previous background estimate $y[n-1]$ as shown below:

$$y[n] = \gamma y[n-1] + (1-\gamma)z[n] \quad (1)$$

This type of exponential smoother is used in Nitzberg [12], Lops [13,14] and [15]. These techniques (namely Clutter Map CFAR or CM-CFAR) average the detector outputs at each resolution cell over several past scans to obtain an estimate of the background power level. In this paper, we apply exponential smoothers to the data collected in the fast-time. It is assumed that background power level of the detector stays at the same level for an extensive period of time, but can have jumps in the power level due to sporadic activities of jammers and other sources. For this purpose, we present a new CFAR method called the Switching IIR CFAR (SIIR CFAR) in which two IIR filters with different rate parameters are utilized to estimate the background level.

The paper is organized as follows. Fundamental information about background estimation using exponential smoothers is given in Section 2. The proposed detector (SIIR CFAR) is described in Section 3. In Section 4, we examine the performance of the suggested method in different scenarios and finally present the conclusions in Section 5.

2. Background estimation via exponential smoothing

We assume that the background returns are Gaussian distributed and undergo square-law detection, possibly after matched filtering. Therefore the magnitude squared range cells, $z[n]$ in Fig. 1, are exponentially distributed with the mean value μ :

$$f_z(z) = \frac{1}{\mu} \exp\left(-\frac{z}{\mu}\right)$$

The output of the system in Fig. 1 can be written as

$$y[n] = (1-\gamma) \sum_{m=0}^{\infty} \gamma^m z[n-m] \quad (2)$$

and the detection threshold is set by

$$T[n] = \alpha y[n-1] \quad (3)$$

where α is the threshold parameter chosen to set the false alarm rate at a desired level [16, p. 264]. It is desired not to include the target returns, whose parameters are not known in general, in the background estimate in order not to bias the system output and to avoid the target self-cancellation. This means that if a target absent decision is made, $z[n]$ is used to update the threshold. Otherwise, the threshold stays constant. The P_{FA} and P_D equations for the described operation are given as, [12],

$$P_{FA} = \frac{1}{\prod_{m=0}^M [1 + \alpha(1-\gamma)\gamma^m]} \quad M \rightarrow \infty \quad (4)$$

$$P_D = \frac{1}{\prod_{m=0}^M [1 + \alpha_D(1-\gamma)\gamma^m]} \quad M \rightarrow \infty \quad (5)$$

where

$$\alpha_D = \frac{\alpha}{1 + \overline{\text{SNR}}} \quad (6)$$

We refer to this method as IIR CFAR in this paper. Even though Eqs. (4) and (5) are widely used in literature, it should be noted that they are not exact. In the derivations given in [12], it is assumed that the threshold value is updated at every step. However, as noted above, the threshold is updated only after a target absent decision is declared. Therefore the rare event of threshold crossing, due to a significant noise realization, is not accounted for in P_{FA} calculations (similarly for P_D). In spite of this fact, the relations provided in [12] are in significant accord with the Monte Carlo simulations and of great practical value. In this paper, we also make use of the same assumption and assume that the filters are always updated. As a side note, we would like to record that faster converging analytical expressions for P_D and P_{FA} of IIR CFAR systems are given in [17]. These relations also follow the same assumption.

The only parameter in IIR CFAR is the update parameter γ . This parameter allows a fraction γ of the previous background estimate to be added to $(1-\gamma)$ times the current cell to form the new estimate. The value of this parameter can be chosen as, [13],

$$\gamma = \frac{N-1}{N+1} \quad (7)$$

With this choice, the parameter N appearing in (7) attains a useful interpretation. When the parameter γ is chosen as such, the steady-state error variance of the exponential smoother is identical to the error variance of a simple averager with N taps. As a result, to mimic the behavior of cell averaging CFAR of, for example 32 cells, one needs to choose $\gamma = 31/33$. It should be noted that the parameter N can be increased indefinitely without any increase in the memory and computation requirements for the IIR CFAR systems.

The performance of IIR CFAR in a homogeneous environment tends to that of the ideal case as $\gamma \rightarrow 1$, [17]. The performance of the IIR CFAR system in the homogeneous environments has been studied in the literature quite extensively but the performance

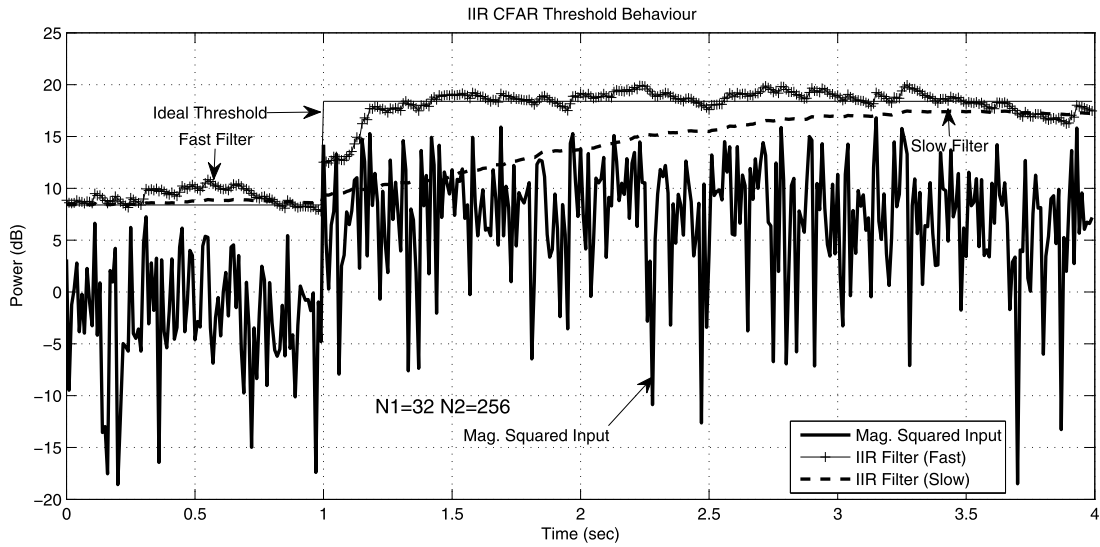


Fig. 2. The CFAR operation with fast and slow IIR filters around a clutter edge. The clutter edge is encountered at $t = 1$ second. The ideal threshold for $P_{FA} = 10^{-4}$ is shown with the solid line.

under nonhomogeneous conditions has not been examined to a similar extent. In a homogeneous background, it is known that the larger the number of cells averaged, the better the background estimate and therefore the detection performance. Conversely, in a nonhomogeneous background, selecting a shorter window provides the advantage of quickly adapting to the nonhomogeneity, yielding a better CFAR performance. The following section describes a technique with two exponential smoothers which attains a good performance in both homogeneous and nonhomogeneous environments through a switching operation via a pre-defined logic.

3. The proposed method

In a homogeneous environment, it is known that as $\gamma \rightarrow 1$ ($N \rightarrow \infty$) the background estimation performance increases. So, for homogeneous environments it is desirable to use a larger N whenever possible. However, for nonhomogeneous environments, it is desirable to use a smaller N so that the performance degrading effect of the nonhomogeneity can be avoided by a faster adaptation. This conflict in the choice of N is illustrated in Fig. 2. In this figure, the data is zero-mean Gaussian distributed and its variance changes at the first second from 0 dB to 10 dB.

In Fig. 2, the threshold estimates of IIR CFAR systems with different rate parameters are shown around a clutter edge. Note that the two IIR CFAR systems shown in Fig. 2 have the same P_{FA} . Here the ‘fast filter’ produces the threshold of $T_1[n]$ and the ‘slow filter’ produces the threshold of $T_2[n]$ as described below:

$$\begin{aligned} T_1[n] &= \alpha_1 y_1[n - 1] \\ T_2[n] &= \alpha_2 y_2[n - 1] \end{aligned} \tag{8}$$

and

$$\begin{aligned} y_1[n] &= \gamma_1 y_1[n - 1] + (1 - \gamma_1)z[n] \\ y_2[n] &= \gamma_2 y_2[n - 1] + (1 - \gamma_2)z[n] \end{aligned} \tag{9}$$

The update parameters γ_1 and γ_2 are given as

$$\gamma_1 = \frac{N_1 - 1}{N_1 + 1} \quad \gamma_2 = \frac{N_2 - 1}{N_2 + 1} \tag{10}$$

In Fig. 2, N_2 is equal to 256, while N_1 is 32. This means that T_2 , in effect, averages more samples and has a larger time constant, hence the name ‘slow filter’ is attributed to this filter. T_1 has a

smaller time constant and can adapt to the environment faster, hence the name ‘fast filter’ is attributed.¹ The aim is to use the slow filter in the homogeneous segments and switch to the fast filter if the statistics of the environment has an abrupt change.

To decide if the environment is homogeneous or not, we adopt the absolute value of the difference between the two filter outputs as the decision logic. In a homogeneous environment, it is expected that both y_1 and y_2 produce outputs in close vicinity of each other. However, an abrupt change in the parameters of the environment results in a rapid change of the fast filter output in comparison to the slow filter. An unexpected deviation in the difference of outputs can be interpreted as an indicator of an abrupt change in the background parameters. If such a change is detected, the system switches to the fast filter and uses the fast filter to estimate the background level. This algorithm is called as Switching IIR CFAR (SIIR CFAR) in this paper.

The event of switching will be based on $|y_1 - y_2|$ as shown in (11)

$$|y_1 - y_2| \begin{cases} \text{use fast filter} \\ \geq T_S \\ \text{use slow filter} \end{cases} \tag{11}$$

where T_S is the switching threshold. Similar to the clean sample rejection rate presented in [18] we suggest False Switching Probability (P_{FS}) for Switching IIR CFAR systems:

$$P_{FS} = P\{|y_1 - y_2| > T_S | \text{homogeneous environment}\} \tag{12}$$

The probability of ‘false switching’ is defined as the probability that a switching decision is made when the environment is in fact homogeneous, that is in the absence of abrupt changes. False switching means that the fast filter is chosen where the slow filter should have been preferred for threshold calculation. Obviously, when P_{FS} is increased, more switching decisions commence. This means that, for larger P_{FS} , the fast filter is used more frequently and the performance of SIIR CFAR algorithm is expected to be closer to that of IIR CFAR with the fast filter. Similarly, for small P_{FS} values, the performance is expected to be similar to that of the slow filter.

An exact derivation for T_S requires an inverse cumulative distribution function (cdf) of $|y_1 - y_2|$. To the best of our knowledge,

¹ Throughout the paper, the filter #1 denotes the fast filter and the filter #2 denotes the slow filter, i.e. we assume that $N_2 > N_1$.

an analytical expression for the distribution of y_1 or y_2 (the exponential smoother outputs) is not available in the literature [13,15]. The distribution of $|y_1 - y_2|$ is even more difficult (due to correlation between y_1 and y_2) and to the best of our knowledge, is not also available in closed form. In the literature, it is common practice to assume y_1 and y_2 to be Gaussian distributed for large N_1 and N_2 as mentioned in [13]. In here, we proceed similarly but improve the conventional Gaussian approximation by providing a further match using the next higher order moments. To this aim, we follow the error correction method given in [19, p. 217]:

$$f_x(x) \approx \frac{1}{\sigma\sqrt{2\pi}} e^{-x^2/2\sigma^2} \left[1 + \frac{m_3}{6\sigma^3} \left(\frac{x^3}{\sigma^3} - \frac{3x}{\sigma} \right) \right] \quad (13)$$

where $x \equiv y_1 - y_2$ and $\sigma^2 = \text{var}\{x\} = m_2$, the second moment of x . To make this error correction, we need the third moment of $y_1 - y_2$, namely $m_3 = E\{(y_1 - y_2)^3\}$. The moments for $n \leq 3$ can be calculated as follows:

$$\begin{aligned} E\{(y_1 - y_2)^n\} &= \sum_{k=0}^n (-1)^k \binom{n}{k} \frac{(1 - \gamma_1)^{n-k} (1 - \gamma_2)^k}{1 - \gamma_1^{n-k} \gamma_2^k} \left(n! \mu^n \sum_{j=0}^n \frac{(-1)^j}{j!} \right) \end{aligned} \quad (14)$$

In terms of N_1 and N_2 (not γ_1 and γ_2) the first three moments of $y_1 - y_2$ are

$$m_1 = 0 \quad (15)$$

$$m_2 = \frac{(N_2 - N_1)^2}{N_1 N_2 (N_1 + N_2)} \mu^2 \quad (16)$$

$$m_3 = \frac{48(N_1 + N_2)(N_1 N_2 - 1)(N_2 - N_1)^3}{(3N_1^2 + 1)(3N_2^2 + 1)(2N_1 N_2 + N_2^2 + 1)(2N_1 N_2 + N_1^2 + 1)} \mu^3 \quad (17)$$

We note that adding more terms to the expression in (13) makes the approximation more accurate but the calculation of higher order moments becomes excessively tedious.

Now, the problem of calculating T_S has been reduced to determining T_S from $P_{FS} = P\{|x| > T_S\}$. Using the approximate pdf in (13) the threshold T_S can be calculated by numerically solving the following equation

$$Q(T_S/\sqrt{m_2}) + \frac{m_3}{\sqrt{8\pi m_2^5}} \exp(-T_S^2/2m_2) \left(\frac{T_S^2 - m_2}{3} \right) = \frac{P_{FS}}{2} \quad (18)$$

where Q is the Gaussian Q function defined as

$$Q(x) = \frac{1}{\sqrt{2\pi}} \int_x^\infty \exp\left(-\frac{u^2}{2}\right) du \quad (19)$$

The steps of derivation for (18) is outlined in Appendix A. To check the fidelity of the suggested approximation, we make the following Monte Carlo simulations. Note that the only parameter required for calculation of T_S is μ (the mean of the magnitude squared observations) which is not available to the system. The goal of the suggested CFAR system is to estimate and track the background noise variance, μ . For comparison purposes, we present three different ways of calculating T_S :

1. $y_1 - y_2$ is assumed to be a normal random variable. For a desired P_{FS} , the switching threshold is found from $T_S = \sqrt{m_2} Q^{-1}(P_{FS}/2)$. Here μ is assumed to be known. This case is called 'Gaussian approximation'.

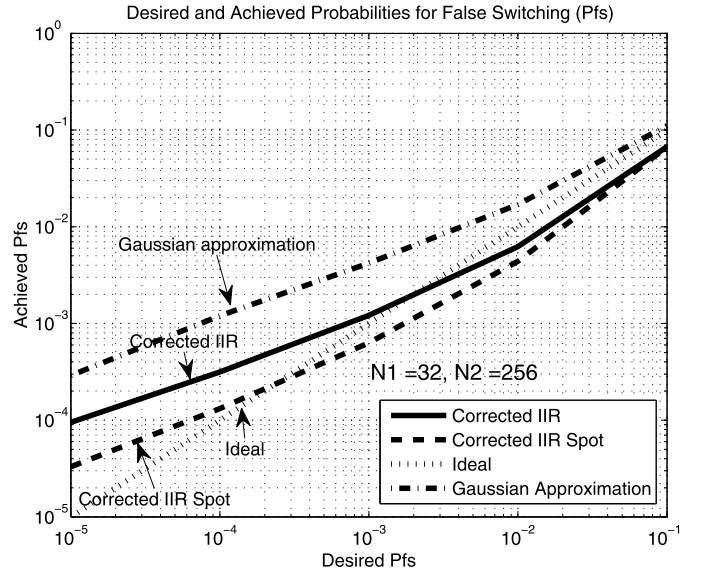


Fig. 3. P_{FS} simulations for $N_1 = 32$ and $N_2 = 256$.

2. For a desired P_{FS} , the threshold T_S is found from (18) and μ is assumed to be known. This case is called 'Corrected IIR'.
3. For a desired P_{FS} , the threshold T_S is found from (18) and μ is assumed to be not known. Since y_1 and y_2 are estimators of noise power, it is assumed that $y_2 = \mu$. Here the slow filter is preferred because of its smaller variance in homogeneous environments. This case is called 'Corrected IIR Spot' since μ is estimated on the spot at each step. It should be noted that this is the case to be used in practice.

The simulation results are seen in Fig. 3. In this figure, the ideal operation, which is the equality of desired and achieved probabilities for false switching, is shown with the straight line of slope 1 and passing through the origin.

Fig. 3 shows that the correction terms given in (13) yield a significant improvement over Gaussian approximation for small false switching probabilities. This means that the switching threshold T_S for (12) can be set using (18) for a wider range of P_{FS} values with the correction.

We would like to note that the numerical solution of (18) for the threshold is a computationally difficult task. It is possible to rewrite (18) in the following form,

$$Q\left(\sqrt{\frac{T_S^2}{m_2}}\right) + c_{N_1, N_2} \exp\left(-\frac{1}{2} \frac{T_S^2}{m_2}\right) \left(\frac{T_S^2}{m_2} - 1\right) = \frac{P_{FS}}{2} \quad (20)$$

where

$$c_{N_1, N_2} = \frac{m_3}{3\sqrt{8\pi m_2^3}} \quad (21)$$

is a constant that depends only on N_1 and N_2 not on μ . We see that (20) is a function of $T_S/\sqrt{m_2}$ or equivalently T_S/μ . To aid the implementation of the threshold selection process, we define the normalized threshold, λ as $\lambda = T_S/\mu$. With this definition, the threshold T_S is the normalized threshold times the background noise variance. Fig. 4 shows the variation of λ for different P_{FS} and (N_1, N_2) values. A system designer can use this graph to set the normalized threshold for a desired P_{FS} . In practice, a look-up table for a specific (N_1, N_2) pair should be prepared and utilized in real-time operation.

The proposed SIIR CFAR algorithm is summarized in Algorithm 1. Here $y_1[n]$ is the fast filter and $y_2[n]$ is the slow filter.

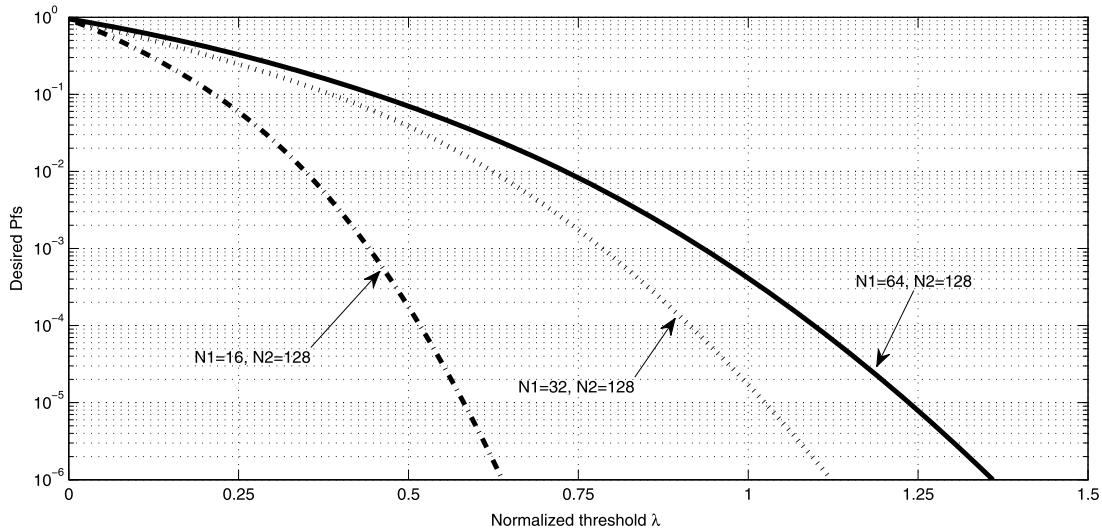


Fig. 4. Normalized threshold λ for different values of (N_1, N_2) .

Algorithm 1 The SIIR CFAR Algorithm

```

Initialize  $y_1[0], y_2[0], T[0]$ 
For a desired  $(N_1, N_2)$  compute  $\gamma_1$  and  $\gamma_2$  from (7)
For a desired  $P_{FA}$  compute  $\alpha_1$  and  $\alpha_2$  from (4)
For a desired  $P_{FS}$  and  $(N_1, N_2)$  lookup  $\lambda$  (or use Fig. 4)
for all  $n > 0$  do
  if  $z[n] < T[n - 1]$  (target is absent) then
     $y_1[n] = \gamma_1 y_1[n - 1] + (1 - \gamma_1) z[n]$ 
     $y_2[n] = \gamma_2 y_2[n - 1] + (1 - \gamma_2) z[n]$ 
  else
     $y_1[n] = y_1[n - 1]$ 
     $y_2[n] = y_2[n - 1]$ 
  end if
  if  $|y_1[n] - y_2[n]| > \lambda y_2[n]$  then
     $T[n] = \alpha_1 y_1[n]$ 
  else
     $T[n] = \alpha_2 y_2[n]$ 
  end if
  Detection decision is based on  $z[n] \underset{H_0}{\overset{H_1}{\geq}} T[n - 1]$ 
end for

```

(i.e. $N_1 < N_2$). $z[n]$ is the magnitude squared input and $T[n]$ is the threshold at time n .

The block diagram of the switching system is given in Fig. 5. In this figure, both filters are always running and the output is switched between two of them depending on the described logic.

The comparator block makes the comparison of $|y_1[n - 1] - y_2[n - 1]| > \lambda y_2[n - 1]$. The output *Select* (S) is 1 if this comparison is true and 0 if it is false. $T[n]$ is switched between the two filter outputs according to S . This concludes the construction of the Switching IIR CFAR algorithm.

We conclude this section with a figure to illustrate the operation of the SIIR CFAR system. Similar to Fig. 2, Fig. 6 shows the operation of the SIIR CFAR around a clutter edge. As seen from this figure, the proposed system switches to the fast filter just after the clutter edge avoiding many false alarms that would be encountered if slow filter was utilized. Fig. 6 is given for illustration purposes and it shows the operation of the system for a single realization. In Section 4, the results of Monte Carlo runs are given to examine the performance of the proposed method in detail.

4. Numerical results

We examine the probability of false alarm and the probability of detection performance of the SIIR CFAR in this section. Our goals

are to illustrate the loss in performance due to false switching in homogeneous environments and to examine the performance (the number of false alarms) just after a clutter edge. We note that the performance loss incurred for the homogeneous case is the cost of performance improvement in the nonhomogeneous case. Our goal is to illustrate this trade-off and examine the effect of different parameters in this trade-off.

4.1. Homogeneous environment

We follow the literature and use a Swerling 1 fluctuating target for the probability-of-detection comparisons. The pdf of $z[n]$ in this case is

$$f_z(z) = \frac{1}{\mu} \exp\left(\frac{-z}{\mu}\right)$$

where

$$\mu = \begin{cases} \beta^2, & \text{under } H_0 \\ \beta^2(1 + \text{SNR}), & \text{under } H_1 \end{cases}$$

where β^2 is the average background noise power which can also be assumed to be equal to 1 with no loss of generalization.

Fig. 7 compares the performance of SIIR CFAR with the optimal detector utilizing known μ . It is observed that the performance of the Switching IIR system is very close to the optimal detector under homogeneous conditions. In this comparison, the slow filter is denoted by IIR(128), an IIR filter tuned to operate so as to average 128 cells, and the fast filter is denoted by IIR(32).

The performance of the switching system can be justified through the following argument: Let the P_D of slow IIR CFAR be denoted by $P_{D,slow}$ and that of fast IIR CFAR by $P_{D,fast}$. In a homogeneous environment, with a probability of P_{FS} the fast filter is selected and with a probability of $1 - P_{FS}$ the slow filter is selected to form the threshold estimate. So, the combined P_D is

$$P_{D,SIIR} = P_{D,fast} P_{FS} + P_{D,slow} (1 - P_{FS}) \approx P_{D,slow} \quad \text{for small } P_{FS} \tag{22}$$

This shows that the combined detection probability is a weighted average of two detection probabilities. Hence the detection probability for the switching system lies in between the two probability curves and it is indeed closer to the curve having the higher detection probability. It has to be noted that in this figure, the false

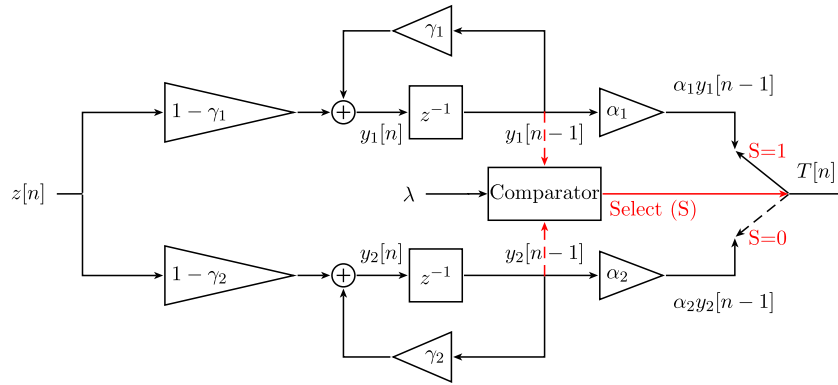


Fig. 5. Block diagram of the proposed system.

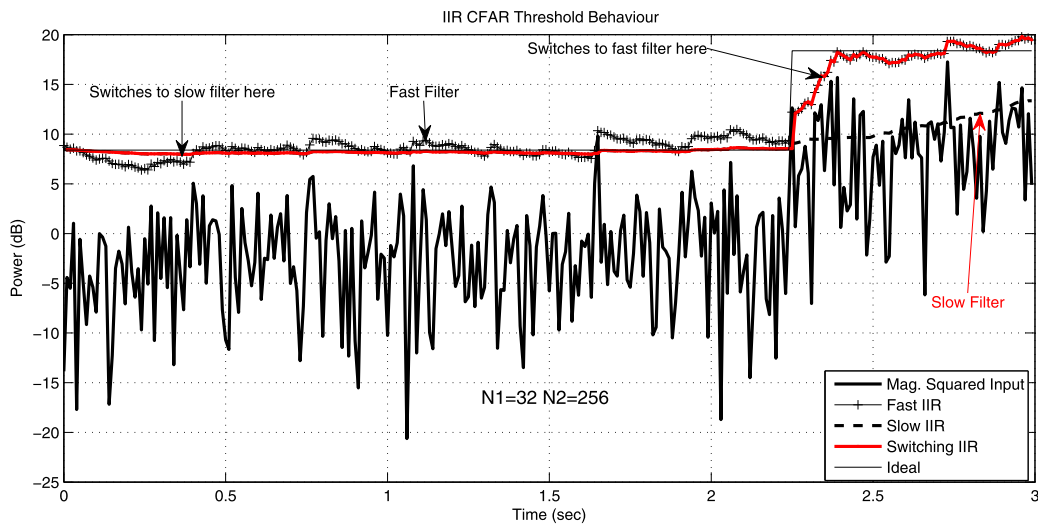


Fig. 6. The operation of switching IIR CFAR around the clutter edge. The clutter edge is encountered at $t = 2$ seconds. The ideal threshold for $P_{FA} = 10^{-4}$ is shown with solid line.

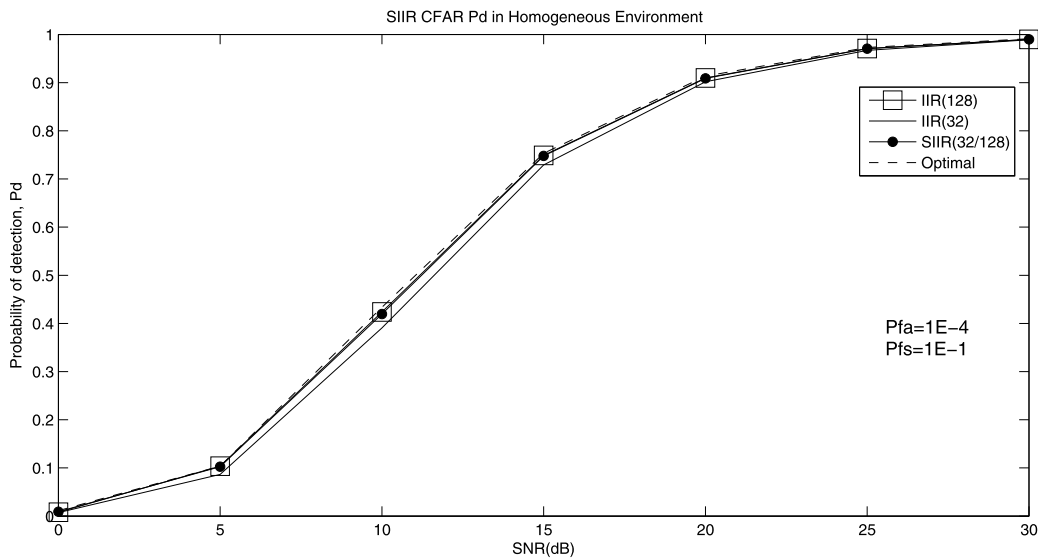


Fig. 7. P_D simulations for $N_1 = 32$, $N_2 = 128$, $P_{FA} = 10^{-4}$, $P_{FS} = 10^{-1}$ under homogeneous conditions.

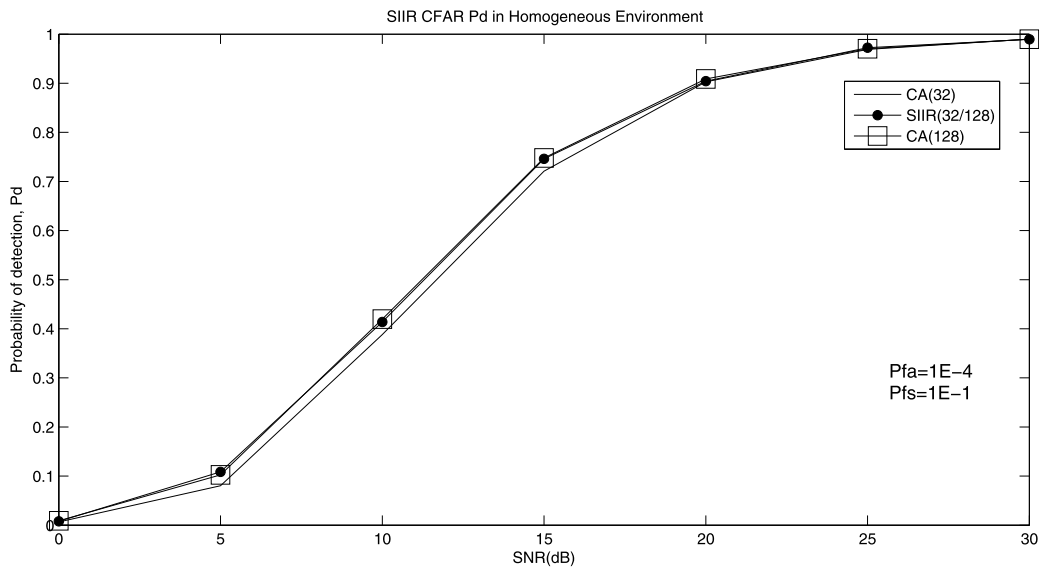


Fig. 8. P_D simulations for $N_1 = 32$, $N_2 = 128$, $P_{FA} = 10^{-4}$, $P_{FS} = 10^{-1}$ under homogeneous conditions vs. CA CFAR.

switching probability has been selected as 0.1 which is a very modest number. As expected, the performance improves when false switching probability is reduced. Simulation results for other parameter values are available in [20].

Next, we compare the SIIR CFAR algorithm with the CA CFAR in homogeneous environment. Fig. 8 shows that the performance of SIIR CFAR is identical to that of CA CFAR in the homogeneous environments. However the computational load and memory requirement of SIIR CFAR is much less than that of CA CFAR.

The conclusion of this section is that SIIR CFAR systems can produce an almost identical performance to cell averaging CFAR in homogeneous environments and there is almost no loss of performance due to switching if the false switching probability is selected low enough.

4.2. Nonhomogeneous environments

We investigate the performance of SIIR CFAR when a clutter edge is present in the reference window. Since IIR filters are causal, the threshold is estimated using the samples in the history; i.e. using the lagging window. By the nature of causal IIR operation, we expect a sudden jump in the false alarm probability just after the clutter edge. The false alarm probability then gradually decreases to the level set by the designer as the process moves into higher variance clutter region.

Fig. 9 shows the P_{FA} performance of IIR(32), IIR(128) and SIIR(32/128) algorithms. As expected, there is a sudden increase in P_{FA} at the clutter transition for all systems.

The merit factor for the presented methods can be the required time after the clutter edge to achieve the desired false alarm probability. IIR(32) has better performance than IIR(128) in this sense because its false alarm rate returns to its steady state value faster than the other. This is because IIR(32) is a faster filter which averages less samples than IIR(128).

The switching operation combines the P_{FA} performance of the slow and fast IIR filters. The SIIR algorithm immediately selects the fast filter which is IIR(32), as soon as the clutter edge is crossed. After a number of range cells beyond the edge, the magnitude of the difference between the fast and slow filters becomes small, and IIR(128) (the slow filter) is reselected.

The effect of the design parameter P_{FS} can also be seen in Fig. 9. For smaller P_{FS} , the slow filter is selected more frequently

therefore the overall false alarm performance is closer to that of the slow filter. The counter statement holds for larger P_{FS} .

Fig. 10 shows the clutter edge P_{FA} performance of CA CFAR vs. SIIR CFAR. It is observed that both SIIR curves (32/64 and 32/128) display a fast recovery towards low P_{FA} values close to that of CA(32) after the clutter edge. On the other hand, it takes somewhat longer to settle at the steady state level at lower P_{FA} values. It can also be stated that SIIR CFAR(32/64) has a performance between CA(32) and CA(64). Similarly, SIIR CFAR(32/128) has a performance lying in between CA(32) and CA(128).

The designer of a typical CA-CFAR system sets the parameter N such that N is sufficiently good at both homogeneous and nonhomogeneous environments (the clutter edge). If N is selected as 32, the performance is good just after the clutter edge (as seen from Fig. 10); but this choice leads to a poorer performance in the homogeneous medium. If N is selected as 64, the performance is poor after the clutter edge (as seen from Fig. 10), but the performance is better at the homogeneous medium due to the utilization of larger number of cells in background estimation. The designer of CA-CFAR system makes a trade-off between two cases and sets the value of N .

The aim of the suggested method is to capture the best characteristics of two CFAR techniques through switching operation. Hence the trade-off point is established through switching.

It should be noted that Fig. 10 contains the comparison of IIR systems (SIIR CFAR) and FIR systems (CA(N) CFAR). Due to the nature of IIR systems, a step-like discontinuity is reflected as an exponential decay in this figure. On the other hand, FIR systems forget all the cells but the latest N cells, that is CA(32) uses only the latest 32 cells for background estimation. This is the reason that CA(32) and CA(64) has an abrupt reduction in the false alarms at the 32nd and 64th cells after the clutter edge.

Fig. 11 shows the clutter edge P_{FA} performance of SIIR CFAR vs. OS CFAR. OS(16/32) and OS(24/32) curves illustrate the performance when the 16th and 24th largest sample in the reference window is taken, respectively, as the background estimate, [22]. As stated in [22], the performance of OS CFAR for homogeneous environment is poorer than the one of CA CFAR. Due to the equivalence of SIIR CFAR with CA CFAR, the proposed system is expected to perform better than OS CFAR under homogeneous environments. For nonhomogeneous environment, it is seen from Fig. 11 that SIIR CFAR has a similar but inferior performance when compared with the OS CFAR. It should be remembered that OS CFAR is a high

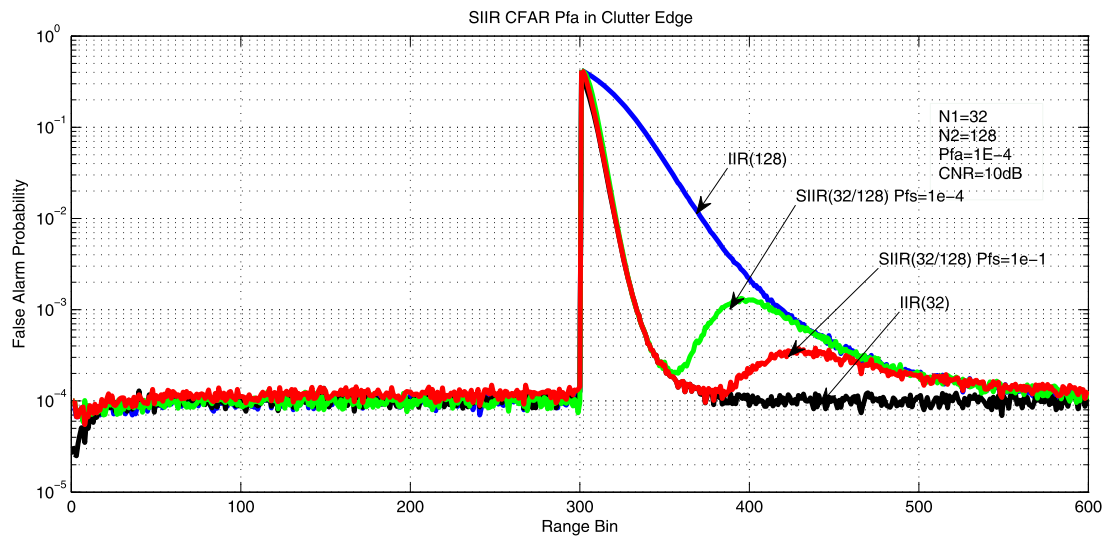


Fig. 9. P_{FA} simulations under clutter edge for $N_1 = 32$, $N_2 = 128$, $P_{FA} = 10^{-4}$, $CNR = 10$ dB, $P_{FS} = 10^{-4}$ and $P_{FS} = 10^{-1}$.

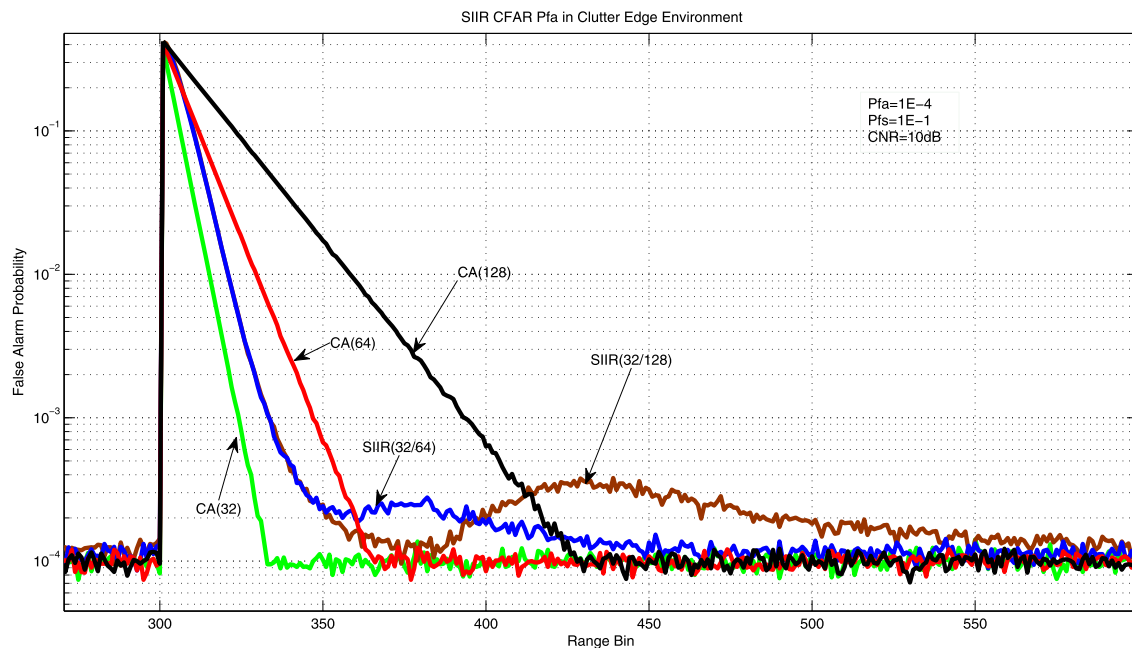


Fig. 10. P_{FA} simulations under clutter edge for SIIR CFAR vs. CA CFAR algorithms.

computation method which cannot be put in the same class with the proposed system from the computational perspective. It should be remembered that our goal in this paper is to present a switching mechanism which enables the successful utilization of simple CFAR techniques. As seen from the block diagram of the proposed scheme given in Fig. 5, the additional computational burden due to proposed switching mechanism is miniscule.

It should also be noted that OS CFAR is particularly valuable for the multiple target scenarios and for the environments with clutter discretely; but not for the clutter edge problem. Given the results of Fig. 11, we believe that an implementation of OS CFAR does have sufficient return to compensate its computational load and therefore is not very rewarding.

5. Conclusions

Conventional CFAR methods use a fixed number of cells to set the threshold and compare the cell under test against the calculated threshold. This can lead to significant memory and com-

putational requirements especially for advanced CFAR systems. In this paper, a novel CFAR processing method using exponential smoothers is presented. In contrast to other methods, the exponential smoothers require much less resources and they are especially suitable for embedded implementations. Proposed method enables the utilization of these computationally attractive structures in nonhomogeneous environments.

A CFAR method based on the utilization of two exponential smoothers with different time-constants is studied. The slow filter is shown to have a better estimation performance in the homogeneous environments, while the fast filter is shown to be superior during the clutter edge transition. A switching mechanism among fast and slow filters is described and the performance of the system with switching, Switching IIR CFAR, is examined.

The performance results show that the Switching IIR CFAR system has negligible performance loss due to false switching in the homogeneous environment. The system has no loss of performance in the multiple target scenarios. The system has some P_{FA} inflation

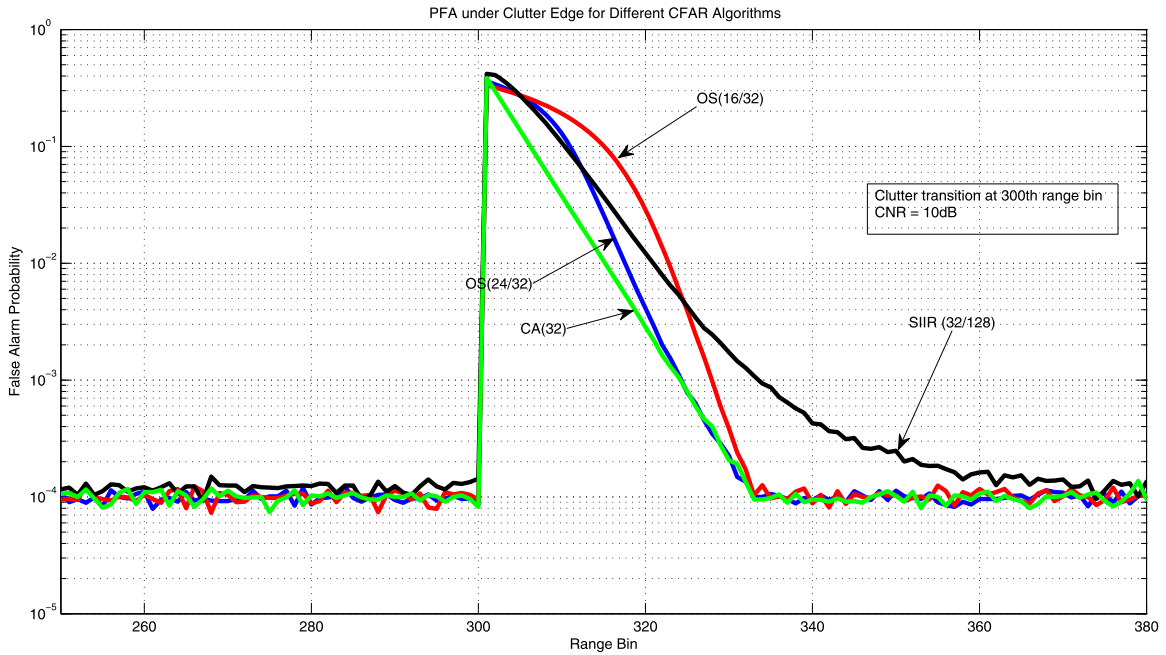


Fig. 11. P_{FA} simulations under clutter edge for SIIR CFAR vs. OS CFAR algorithms.

just after the clutter edge, but it can be controlled by adjusting the parameters (N_1 , N_2 and P_{FS}) of the proposed system. The proposed method provides a mechanism with a few parameters to establish a trade-off between the conflicting requirements of homogeneous and nonhomogeneous environments.

Appendix A. Derivation of Eq. (18)

Here we outline the derivation of Eq. (18). The false switching event is defined as follows:

$$P_{FS} = P\{|x| > T_S\} = 2P\{x > T_S\} = 2 \int_{T_S}^{\infty} f_x(x) dx \quad (A.1)$$

where $x = y_1 - y_2$. In the definition above, $P\{x > T_S\}$ and $P\{x < -T_S\}$ are taken as equal to each other. It should be noted that x is zero mean random variable with other moments given in (16) and (17). Since the third moment is not equal to zero, we cannot immediately say that $P\{x > T_S\} = P\{x < -T_S\}$. But since $N_2 > N_1$; this leads the random variable x to skew towards positive x-axis. Therefore taking $P\{x > T_S\} = P\{x < -T_S\}$ is a pessimistic assumption which can lead to more false alarms than designed. Fig. 3 indeed confirms this.

When the approximation of $f_x(x)$ given in (13) is substituted in (A.1) we get,

$$\begin{aligned} \frac{P_{FS}}{2} &= \int_{T_S}^{\infty} \frac{1}{\sigma\sqrt{2\pi}} e^{-\frac{x^2}{2\sigma^2}} + \int_{T_S}^{\infty} \frac{1}{\sigma\sqrt{2\pi}} e^{-\frac{x^2}{2\sigma^2}} \frac{m_3 x^3}{6\sigma^6} \\ &\quad - \int_{T_S}^{\infty} \frac{1}{\sigma\sqrt{2\pi}} e^{-\frac{x^2}{2\sigma^2}} \frac{m_3 x}{2\sigma^4} \end{aligned} \quad (A.2)$$

When the first integral on the right side of (A.2) is expressed in terms of $Q(\cdot)$ function and the second and third integrals are evaluated using [21, p. 108], we get the relation presented in (18).

References

- [1] H. Finn, Adaptive detection in clutter, in: Fifth Symposium on Adaptive Processes, vol. 5, 1966, pp. 562–567.
- [2] J. Rickard, G. Dillard, Adaptive detection algorithms for multiple-target situations, IEEE Trans. Aerospace Electron. Syst. 13 (1977) 338–343.
- [3] H. Finn, A CFAR design for a window spanning two clutter fields, IEEE Trans. Aerospace Electron. Syst. 22 (1986) 155–169.
- [4] H. Rohling, Radar CFAR thresholding in clutter and multiple target situations, IEEE Trans. Aerospace Electron. Syst. 19 (1983) 608–621.
- [5] S. Himonas, M. Barkat, Automatic censored CFAR detection for nonhomogeneous environments, IEEE Trans. Aerospace Electron. Syst. 28 (1992) 286–304.
- [6] M. Smith, P. Varshney, VI-CFAR: a novel CFAR algorithm based on data variability, in: IEEE National Radar Conference, 1997, pp. 263–268.
- [7] A. Farrouki, M. Barkat, Automatic censoring CFAR detector based on ordered data variability for nonhomogeneous environments, IEE Proc. Radar Sonar Navig. 152 (2005) 43–51.
- [8] A. Farrouki, M. Barkat, Automatic censored mean level detector using a variability-based censoring with non-coherent integration, Signal Process. 87 (2007) 1462–1473.
- [9] S. Leung, J. Minett, CFAR data fusion using fuzzy integration, in: Proceedings of the Fifth IEEE International Conference on Fuzzy Systems, vol. 2, 1996, pp. 1291–1295.
- [10] Z. Hammoudi, F. Soltani, Distributed CA-CFAR and OS-CFAR detection using fuzzy spaces and fuzzy fusion rules, IEE Proc. Radar Sonar Navig. 151 (2004) 135–142.
- [11] A. Zaimbashi, Y. Norouzi, Automatic dual censoring cell-averaging CFAR detector in non-homogenous environments, Signal Process. 88 (2008) 2611–2621.
- [12] R. Nitzberg, Clutter map CFAR analysis, IEEE Trans. Aerospace Electron. Syst. 22 (1986) 419–421.
- [13] M. Lops, M. Orsini, Scan-by-scan averaging CFAR, IEE Proc. Radar Signal Process F 136 (1989) 249–254.
- [14] M. Lops, Hybrid clutter-map/L-CFAR procedure for clutter rejection in nonhomogeneous environment, IEE Proc. Radar Sonar Navig. 143 (1996) 239–245.
- [15] X. Meng, Performance analysis of Nitzberg’s clutter map for Weibull distribution, Digit. Signal Process. 20 (2010) 916–922.
- [16] N. Levanon, Radar Principles, Wiley-Interscience, 1988.
- [17] N. Levanon, Numerically efficient calculations of clutter map CFAR performance, IEEE Trans. Aerospace Electron. Syst. 23 (1987) 813–814.
- [18] J. Lehtomaki, M. Juntti, H. Saarnisaari, CFAR strategies for channelized radiometer, IEEE Signal Process. Lett. 12 (2005) 13–16.
- [19] A. Papoulis, Probability, Random Variables, and Stochastic Processes, 4th edn., McGraw-Hill Higher Education, 2002.
- [20] B. Gurakan, CFAR processing with multiple exponential smoothers for non-homogeneous environments, M.Sc. thesis, Middle East Technical University, 2010.
- [21] I. Gradshteyn, I. Ryzhik, Table of Integrals, Series, and Products, 5th edn., Academic Press, 1994.

- [22] P. Gandhi, S. Kassam, Analysis of CFAR processors in homogeneous background, *IEEE Trans. Aerospace Electron. Syst.* 24 (1988) 427–445.

Berk Gurakan has received his B.S. ('08) and M.S. ('10) degrees in Electrical and Electronics Engineering from Middle East Technical University, Ankara, Turkey. He is currently pursuing his Ph.D. studies in University of Maryland, College Park, Maryland, USA. His research interests are signal processing, wireless communications and networking.

Çağatay Candan has received his B.S. degree from Middle East Technical University, Ankara, Turkey ('96); M.S. degree from Bilkent University, Ankara, Turkey ('98) and Ph.D. degree from Georgia Institute of Technology, Atlanta, USA ('04). He is currently an associate professor at the Department of Electrical and Electronics Engineering, Middle East

Technical University. His research interests are statistical signal processing (with an emphasis on detection and estimation) and its applications.

Tolga Çiloğlu received his B.S. ('85), M.S. ('87) and Ph.D. ('94) degrees in Electrical and Electronics Engineering from Middle East Technical University, Ankara, Turkey. He is currently a professor at the Department of Electrical and Electronics Engineering, Middle East Technical University. His research interests are adaptive and statistical processing, speech processing, pattern recognition and digital filter design. In particular, he has been involved in research and industrial projects on underwater acoustic systems (detection, tracking, source localization), speech modeling (acoustic, prosodic), speech enhancement, speech synthesis and recognition, sleep sound analysis, active noise control and discrete coefficient filter design.